Electron Spin Resonance and Electron Spin Echo Modulation Evidence for the Isomorphous Substitution of Ti in TAPO-5 Molecular Sieve

A. M. Prakash, Vadim Kurshev, and Larry Kevan*

Department of Chemistry, University of Houston, Houston, Texas 77204

Received: August 1, 1997; In Final Form: September 23, 1997[⊗]

New evidence for the isomorphous substitution of titanium into titanium aluminophosphate molecular sieve of structure type AFI (TAPO-5) is reported by combined electron spin resonance (ESR) and electron spin echo modulation (ESEM) spectroscopic studies. Synthesized TAPO-5 and TiO_2/SAPO-5 materials are compared. These materials were activated and then reduced by γ-irradiation at 77 K or by CO at ambient to high temperatures. γ-irradiation at 77 K of TAPO-5 produces an ESR signal characterized by $g_1 = 1.965$, $g_2 = 1.920$, and $g_3 = 1.879$ best explained as arising from trivalent titanium at a framework site together with a strong signal due to V centers. γ-irradiation of TiO_2/SAPO-5 gives an ESR signal with $g_\perp = 1.971$ and $g_\parallel = 1.907$ typical of Ti(III) in octahedral symmetry. Upon CO reduction TAPO-5 gives a spectrum with rhombic g parameters $g_1 = 1.969$, $g_2 = 1.954$, and $g_3 = 1.923$, which are different from the corresponding parameters of the Ti(III) species produced by γ-irradiation. CO reduction of TiO_2/SAPO-5 produces an ESR signal with similar axial g parameters as observed for the Ti(III) species produced after γ-irradiation. These differences in behavior between the two materials are best explained in terms of additional coordination of tetrahedral framework Ti by CO in TAPO-5, while octahedral Ti in TiO_2/SAPO-5 is incapable of further coordination with CO. ^{31}P ESEM for the tetrahedral Ti(III) species in TAPO-5 obtained by γ-reduction shows one phosphorus atom at 3.9 Å and two phosphorus atoms at 4.8 Å, which supports that titanium substitutes for a framework phosphorus site. Strong ^{27}Al modulation is observed for this Ti(III) signal, which further confirms the closer proximity of the Ti ions to framework aluminum than to phosphorus.

Introduction

Titanium compounds have been widely used as catalysts in the selective oxidation of various organic substrates. The discovery of the remarkable catalytic activity of titanium silicates-1 (TS-1) in selectively oxidizing a wide range of organic compounds in the presence of hydrogen peroxide has triggered intensive research in the area of synthesis of titanium-based molecular sieves for catalysis.[1] Several new titanium-containing molecular sieves have been synthesized including TS-2 (MEL),[2] Ti−ZSM-48,[3] Ti−β(BEA),[4] titanium aluminophosphates such as TAPO-5 (AFI),[5] TAPO-11 (AEL),[5] and TAPO-36 (ATS),[6] and titanium-containing mesoporous molecular sieves such as Ti−MCM-41[7] and Ti−MCM-48.[8] Recently, new microporous titanosilicates, named ETS-4 and ETS-10, where titanium has six coordination have been reported.[9,10]

Electron spin resonance (ESR) spectroscopy has been widely used for characterizing transition-metal ions incorporated into molecular sieves.[11] ESR evidence for framework substitution of Ti in TS-1 has been reported.[12] However, framework substitution of Ti in other Ti-containing molecular sieves has not been studied by ESR. The pulsed ESR technique known as electron spin echo modulation (ESEM) spectroscopy has been very effectively employed for identifying and locating transition-metal ions such as Cu, Ni, Pd, Mn, etc., in molecular sieves modified by these ions.[13] However, ESEM has not yet been applied to the location of Ti in Ti-based molecular sieves.

TAPO-5 is a large pore titanium-containing aluminophosphate molecular sieve with a unidimensional pore structure and hexagonal symmetry. Isomorphous substitution of Ti in TAPO-5 has been suggested primarily from powder X-ray analyses showing an increase in unit cell parameters with an increase in the amount of Ti.[5,6] Here we report the first ESR and ESEM studies on TAPO-5 molecular sieve to provide direct evidence for framework substitution of Ti in AlPO-5 molecular sieve.

Experimental Section

Synthesis. The synthesis procedure used in the preparation of TAPO-5 is essentially same as that reported by Ulgappan and Krishnasamy.[5] The optimized gel composition was 1.0 R:0.1 TiO_2:1.0 Al_2O_3:1.0 P_2O_5:40 H_2O, where R is triethylamine. In a typical synthesis 27.8 g of aluminum isopropoxide (Aldrich, 98%) was slurred in 37 g of deionized water. The slurry was stirred for 3 h. A second solution was prepared by mixing 2.3 g of titanium butoxide (Aldrich, 98%) and 15.4 g of phosphoric acid (Aldrich, 85%) diluted with 9 g of water. To this solution was added 2.5 mL of aqueous H_2O_2 (Merck, 30%). The resulting clear orange solution was added dropwise to the alumina slurry followed by 6.7 g of triethylamine. The final gel was stirred for 30 min before loading into a 100 cm^3 stainless steel autoclave lined with poly(tetrafluoroethylene). The pH of the gel was 6. Crystallization was done at 460 K for 24 h in an air oven without agitation. After crystallization the product was separated from the mother liquor, washed with water, and dried at 340 K overnight. Samples of AlPO-5 and SAPO-5 were synthesized following the procedures reported in the literature.[14] All the as-synthesized samples were calcined by raising the temperature slowly to 823 K in flowing N_2 and keeping the sample at this temperature for 16 h in flowing O_2 for removal of the organic template.

The TiO_2/SAPO-5 composite material was prepared by a procedure essentially similar to that reported for TiO_2/X, TiO_2/Y, and TiO_2/MCM-41 composite materials.[15] A titania sol where the TiO_2 particle size is about 2−4 nm was prepared by the controlled hydrolysis of titanium isopropoxide in the presence of ethanol and nitric acid at 277 K and maintained at this temperature for 10 h with stirring. Then 1.5 g of calcined

[⊗] Abstract published in *Advance ACS Abstracts,* November 1, 1997.

S1089-5647(97)02521-2 CCC: $14.00 © 1997 American Chemical Society

SAPO-5 was added to 100 mL of the clear transparent titania sol, and the mixture was stored in a refrigerator at 277 K for 3 days with occasional shaking. The solvent was removed from the final suspension by filtration, and the solid was then dried in an air oven at 343 K overnight.

Sample Treatment and Measurements. X-ray powder diffraction patterns were recorded on a Philips PW 1840 diffractometer using Cu Kα radiation. Chemical analysis of the samples was carried out by electron microprobe analysis on a JEOL JXA-8600 spectrometer.

For ESR and ESEM studies, the calcined samples were loaded into 3 mm o.d. by 2 mm i.d. Suprasil quartz tubes and evacuated to a final pressure of 10^{-4} Torr. Calcined samples were dehydrated in vacuum by gradually raising the temperature from room temperature to 673 K over a period of 6 h and kept at that temperature for 24 h. The dehydrated samples were then treated with 600 Torr of O_2 at 773 K for 8 h followed by evacuation at this temperature. The samples were then exposed to γ-radiation from a ^{60}Co source at 77 K to a total dose of 0.93 Mrad at a dose rate of 0.20 Mrad h^{-1}. ESR spectra were taken after each treatment to monitor any change that may occur in the samples. ESR spectra were recorded with a Bruker ESP 300 X-band spectrometer at 77 K. The magnetic field was calibrated with a Varian E-500 gaussmeter. The microwave frequency was measured by a Hewlett- Packard HP 5342A frequency counter. ESEM spectra were measured at 4.8 K with a Bruker ESP 380 pulsed ESR spectrometer. Three pulse echoes were measured by using a $\pi/2-\tau-\pi/2-T-\pi/2$ pulse sequence as a function of time T to obtain the time domain spectrum. Both the theory and methods used for ESEM measurements and simulation of the data are described in detail elsewhere.[16] To minimize ^{27}Al modulation from framework aluminum in measurements of ^{31}P modulation, the interpulse time τ was fixed accordingly, depending on the magnetic field position. The phosphorus modulation was analyzed by a spherical approximation for powder samples in terms of N nuclei at distance R with an isotopic hyperfine coupling A_{iso}.[16] The best fit simulation of an ESEM signal is found by varying the parameters until the sum of the squared residuals is minimized.

Results

X-ray diffraction patterns of both as-synthesized and calcined TAPO-5 confirm well-crystallized samples of the AFI structure. No impurity phase was detected. Electron microprobe analysis gave framework chemical compositions of $(Al_{0.5}P_{0.5})O_2$, $(Si_{0.04}Al_{0.49}P_{0.47})O_2$, and $(Ti_{0.02}Al_{0.5}P_{0.48})O_2$ respectively for AlPO-5, SAPO-5, and TAPO-5. The composition for TAPO-5 suggests that titanium substitutes for framework phosphorus. A similar conclusion was made by Zahedi-Niaki et al.[6] from the chemical analysis of their TAPO-5 sample prepared in the presence of TPAOH. In SAPO-5, the composition suggests that while a fraction of silicon substitutes for Al−P pairs, the majority substitutes for phosphorus.

Following removal of the template by calcination in O_2 at 773 K, TAPO-5 sample shows no ESR signal at room temperature or 77 K. Again, no ESR signal is observed when a calcined sample is dehydrated at 673 K under vacuum or after O_2 treatment at 773 K. However, an ESR signal with a rhombic **g** tensor with $g_1 = 1.965$, $g_2 = 1.920$, and $g_3 = 1.879$ is observed after γ-irradiation at 77 K (Figure 1). The sample was annealed at 295 K for 30 s before recording the spectrum in Figure 1. As will be discussed later, we assign this signal to Ti(III) produced by the reduction of Ti(IV) by γ-irradiation. The considerable departure of the g components from g_e reflects an appreciable spin−orbit interaction for this species. As shown in the inset of Figure 1, a second strong signal with $g_1 = 2.020$, $g_2 = 2.006$, and $g_3 = 1.994$ due to V centers is also observed after γ-irradiation.[17] In addition to these signals, the original spectrum recorded before annealing at room temperature contains a doublet separated by ∼500 G due to trapped H atoms.[18] This signal vanishes immediately upon exposure to room temperature for a short duration (30 s).

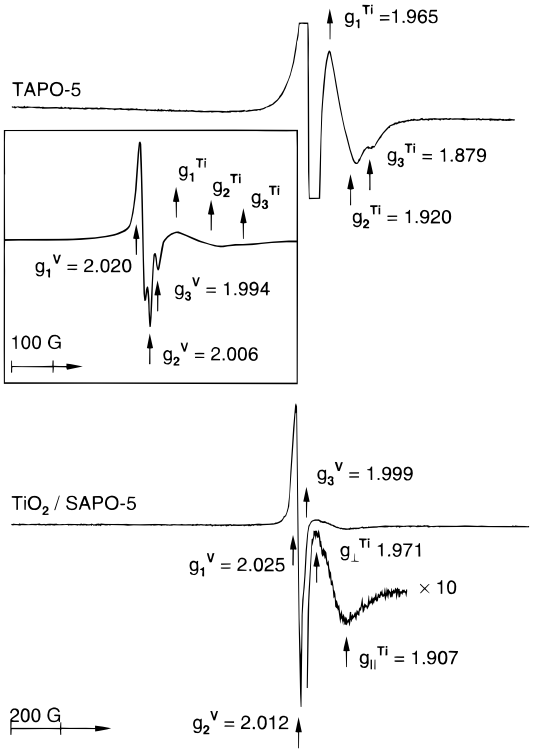

Figure 1. ESR spectra at 77 K of TAPO-5 (top) and TiO_2/SAPO-5 (bottom) after γ-irradiation at 77 K of dehydrated samples. The inset shows the spectrum for TAPO-5 at low receiver gain.

TiO_2/SAPO-5 also does not show any ESR signal after dehydration. A weak ESR signal with an axial **g** tensor with $g_\perp = 1.971$ and $g_{||} = 1.907$ is observed after γ-irradiation of a dehydrated sample at 77 K (Figure 1). A similar signal has been observed for Ti(III) in materials where Ti has distorted octahedral symmetry.[19] A strong signal with $g_1 = 2.025$, $g_2 = 2.012$, and $g_3 = 1.999$ due to V centers is also observed. A doublet due to atomic hydrogen is also observed before annealing to room temperature.

For comparison, samples of AlPO-5 and SAPO-5 were studied by ESR after exposure to γ-irradiation. Figure 2 shows the ESR spectra observed for these samples after dehydration at 673 K for 12 h and subsequent γ-irradiation at 77 K. AlPO-5 shows a relatively weak ESR signal with $g_1 = 2.020$, $g_2 = 2.006$, and $g_3 = 1.994$ besides a doublet signal due to atomic hydrogen. SAPO-5 shows a rhombic signal with $g_1 = 2.025$, $g_2 = 2.011$, and $g_3 = 1.999$ which is much stronger than the signal in AlPO-5. These signals observed in AlPO-5 and SAPO-5 are also found in TAPO-5 and TiO_2/SAPO-5. The doubly integrated relative intensity of this signal is approximately 1:17:33 for AlPO-5, SAPO-5, and TAPO-5, respectively.

When a dehydrated sample of TAPO-5 is exposed to CO (10 Torr) and the temperature is increased, an ESR signal appears, and its intensity increases as the temperature increases. Figure 3 shows a typical ESR signal obtained under 10 Torr of CO heated at 573 K for 30 min. The maximum intensity of the signal is reached around that temperature. This ESR signal has $g_1 = 1.969$, $g_2 = 1.954$, and $g_3 = 1.923$.

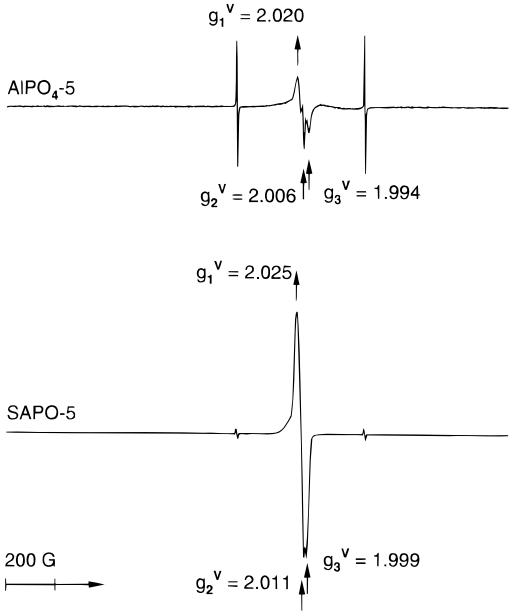

Figure 2. ESR spectra at 77 K of AlPO-5 (top) and SAPO-5 (bottom) after γ-irradiation at 77 K of dehydrated samples.

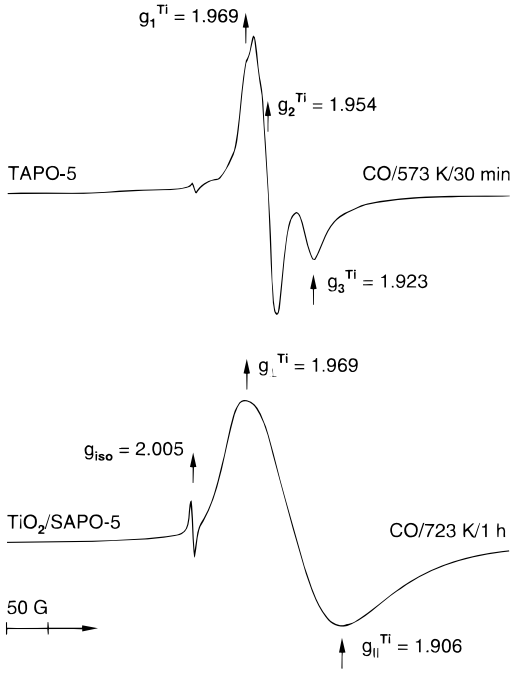

Figure 3. ESR spectra at 77 K of TAPO-5 (top) and TiO_2/SAPO-5 (bottom) after CO reduction of dehydrated samples.

In contrast, when TiO_2/SAPO-5 is exposed to 10 Torr of CO, an isotropic ESR signal with $g = 2.005$ is observed at 295−573 K after 30 min exposure at each temperature. However, when the temperature is raised above 573 K, an axial ESR signal starts developing. The intensity of this signal reaches a maximum around 723 K. Figure 2 shows a typical signal after exposure to 10 Torr of CO at 723 K for 1 h. The ESR spectrum is axially symmetric with $g_\perp = 1.969$ and $g_\parallel = 1.906$. Note that the g values of this signal are the same as observed for TiO_2/SAPO-5 after γ-irradiation, thus confirming that reduction by both γ-irradiation and CO exposure produce the same Ti species.

The reaction between molecular oxygen and TAPO-5 and TiO_2/SAPO-5 after CO exposure was also studied. The samples were evacuated at room temperature before exposing to 10 Torr of O_2 at 295 K. Strong ESR signals are observed immediately after O_2 exposure. Figure 4 shows the ESR spectra for TAPO-5 and TiO_2/SAPO-5 after reaction with O_2 for 30 min at 295 K. The ESR signal intensities decrease as the samples are annealed to higher temperatures and vanish completely at 573 K. These signals can be reproduced only after evacuation and subsequent reduction with CO followed by exposure to oxygen. The TAPO-5 signal has $g_1 = 2.025$, $g_2 = 2.013$, and $g_3 = 2.007$, and the TiO_2/SAPO-5 signal has $g_1 = 2.018$, $g_2 = 2.013$, and $g_3 = 2.006$. The observed **g** tensor components are consistent with the values reported for O_2^-.[20] Note that while the g_2 and g_3 components are essentially same for the two samples, the g_1 components are slightly different.

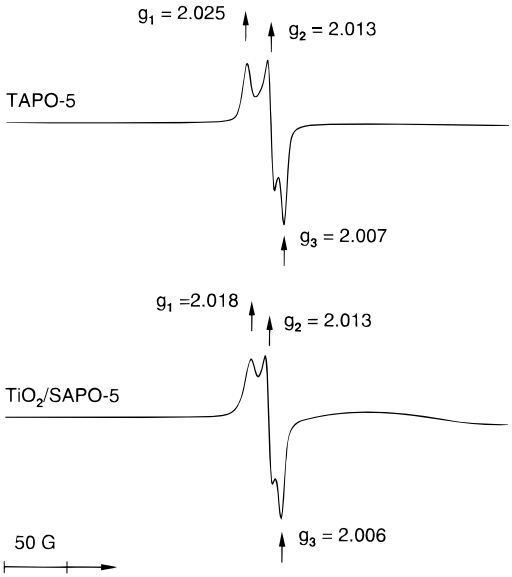

Figure 4. ESR spectra at 77 K of TAPO-5 (top) and TiO_2/SAPO-5 (bottom) after CO reduction, evacuation, and oxygen treatment at 295 K for 30 min.

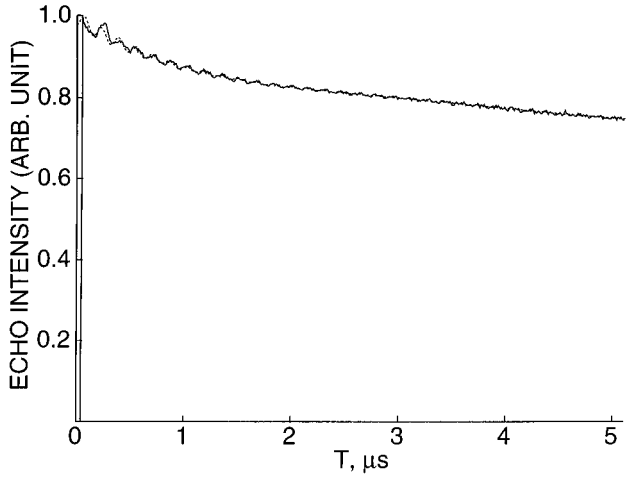

Figure 5. Experimental (—) and simulated (···) three-pulse ^{31}P ESEM spectra of γ-irradiated TAPO-5 at the magnetic field corresponding to g_2 of the Ti(III) species.

ESEM measurements of ^{31}P and ^{27}Al modulation of Ti species produced by γ-ray reduction in TAPO-5 provide convincing evidence for framework substitution of the titanium. Figure 5 shows the experimental and simulated three-pulse ^{31}P ESEM patterns recorded at $\tau = 0.25$ μs to suppress the modulation from framework aluminum. The magnetic field was selected at g_2 of the Ti(III) species (Figure 1). Simulation of the spectrum shows one nearest-neighbor phosphorus at 3.9 Å and two next-nearest phosphorus at 4.8 Å. As will be discussed below, these parameters can be interpreted in terms of Ti

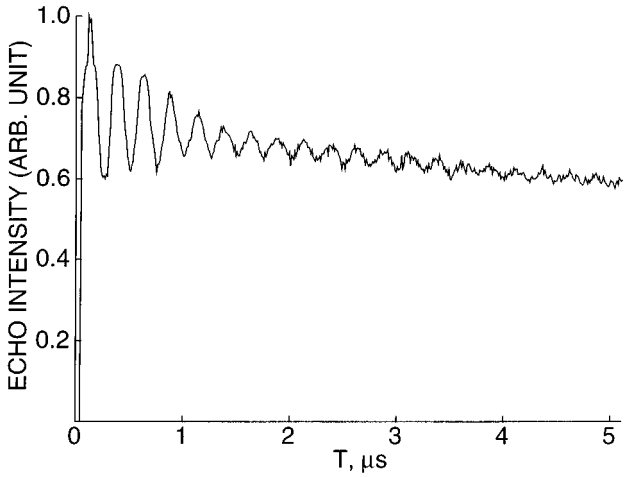

Figure 6. Experimental three-pulse ^{27}Al ESEM spectrum of γ-irradiated TAPO-5 at the magnetic field corresponding to g_2 of the Ti(III) species.

substituted for a framework phosphorus. The ^{27}Al modulation pattern of Ti observed for TAPO-5 provides additional evidence for this conclusion.

^{27}Al modulation of Ti species was measured at the same magnetic field as that used for ^{31}P modulation. The interpulse time τ was selected as 0.12 μs to minimize ^{31}P modulation. Figure 6 shows the ^{27}Al ESEM pattern recorded for TAPO-5. Although quantitative simulation of the aluminum modulation was not undertaken due to its large quadrupole interaction which adds two to three additional fitting parameters, the strong aluminum modulation observed for TAPO-5 clearly indicates the close proximity of the paramagnetic Ti(III) to framework aluminum.

ESEM measurements on TiO_2/SAPO-5 after γ-irradiation show neither ^{31}P nor ^{27}Al modulation. This suggests that these nuclei are at distances greater than about 7 Å from the paramagnetic Ti(III).

Discussion

The synthesis of titanium-based molecular sieves where titanium is believed to be isomorphously substituted for framework atoms has been pursued vigorously for the past several years because of the interesting catalytic properties exhibited by these materials. Although several materials have resulted from these collective efforts, the exact site and coordination of titanium have not typically been characterized. The isomorphous substitution of titanium in TS-1 at a framework tetrahedral site has been confirmed.[1] Convincing evidence for tetrahedral titanium in TS-1 has been provided by analysis of ESR spectra observed upon the reduction of TS-1 with CO and subsequent reaction with O_2.[12] An axially symmetric ESR signal with two $g_{\|}$ lines at 1.98 and 1.97 and one $g_{\perp}$ line at 1.913 was observed upon CO treatment of an evacuated TS-1 sample. These signals have been assigned to Ti(III) in two tetrahedral environments produced by reduction of T(IV) by CO. The subsequent addition of O_2 produces a new signal identified as O_2^- at the expense of Ti(III). This behavior of TS-1 was then compared with the behavior of similarly treated Ti-exchanged ZSM-5 where Ti is in extraframework sites. An axially symmetric signal with $g_{\perp} = 1.97$ and $g_{\|} = 1.94$ consistent with Ti(III) in distorted octahedral coordination was observed. The O_2^- superoxide ion produced on this exchanged material by O_2 treatment has one of its g components different from the corresponding component of O_2^- produced on TS-1.

γ-irradiation of TAPO-5 produces two ESR signals with three g components. The strong signal with $g_1 = 2.020$, $g_2 = 2.006$, and $g_3 = 1.994$ is assigned to V centers (hole centers) created by the radiation since a similar signal is observed in AlPO-5 upon the same treatment. V centers have been studied thoroughly in zeolites as well as in other materials.[17,21] In zeolites two V centers associated with Al−O−Si and Si−O−Si units of the framework have been reported.[17] These are radiation-induced hole centers trapped in the lone-pair p orbital of the associated oxygen atoms. We assign the second rhombic signal with $g_1 = 1.965$, $g_2 = 1.920$, and $g_2 = 1.879$ to Ti(III) produced by reduction of Ti(IV) by γ-irradiation. This is supported by the fact that no similar species is produced in AlPO-5 or SAPO-5 so it is improbable that this species is associated with framework phosphorus or aluminum. By the same reasoning, the species cannot be assigned to NO or NO_2 molecules or any carbonaceous paramagnetic species that might reasonably be formed during removal of the organic template by calcination. Furthermore, all these inorganic paramagnetic species have characteristic ESR spectra.[22,23]

The ESR spectrum for TiO_2/SAPO-5 after γ-irradiation is different from that for TAPO-5. The rhombic signal with $g_1 = 2.025$, $g = 2.012$, and $g = 1.999$ can be again assigned to V centers produced in SAPO-5. The second axial signal with $g_{\perp} = 1.971$ and $g_{\|} = 1.907$ can be assigned to Ti(III) produced by reduction of Ti(IV). Similar species have been observed for Ti(III) in rutile TiO_2 as well as in several TiO_2 supported silicas.[19,24] The symmetry of the titanium species in these materials is distorted octahedral. Similar ESR signals with slightly different **g** tensors have been observed for Ti(III) in Ti-exchanged ZSM-5 zeolite[12] in which the Ti is assigned to trivalent coordination at ion exchange sites.

The **g** tensor of Ti(III) in TAPO-5 is different from that for Ti (III) in TS-1[12] and for Ti(III) in ETS-10.[25] If titanium in TAPO-5 occupies framework sites, one expects tetrahedral site symmetry in dehydrated TAPO-5. However, Ti may have additional coordination with extraframework species in as-synthesized or hydrated TAPO-5. The rhombic **g** tensor for Ti(III) in TAPO-5 together with the fact that this tensor is different from that for TS-1 suggests a distorted environment for this ion. As for other titanosilicate molecular sieves, the presence of a very small amount of extraframework titanium as TiO_2 nanoparticles in TAPO-5 is always a possibility. Distinguishing a trace TiO_2 phase from framework titanium species by ESR does not seem possible due to spectral overlap.

It has been observed that the stability of V centers in zeolites strongly depends on the presence of electron scavengers such as H^+.[17] This is found to be the true in the present case also. The V centers produced in SAPO-5 are more intense than the V centers in AlPO-5, and the concentration of V centers in TAPO-5 is almost double that in SAPO-5. A reaction mechanism for the formation of V centers in aluminosilicate zeolites has been proposed by Abou-Kais et al.[17] Following this interpretation for zeolites, a mechanism for V center formation in AlPO-5, SAPO-5, and TAPO-5 molecular sieves is proposed in Scheme 1.

This mechanism is consistent with an increase in V center intensity in SAPO-5 and TAPO-5. The AlPO framework is not an electron scavenger, and it is probable that the ejected electron readily neutralizes newly created V centers and shifts the equilibrium toward the left to give a low V center concentration (mechanism I). On the other hand, H^+ ions are good electron scavengers and can readily react with the ejected electron to form H atoms. However, the H atoms are unstable and may be trapped in some cavities or recombine with the V centers. Thus, the large increase in V centers in SAPO-5 and TAPO-5 in comparison with AlPO-5 can be explained by the

SCHEME 1

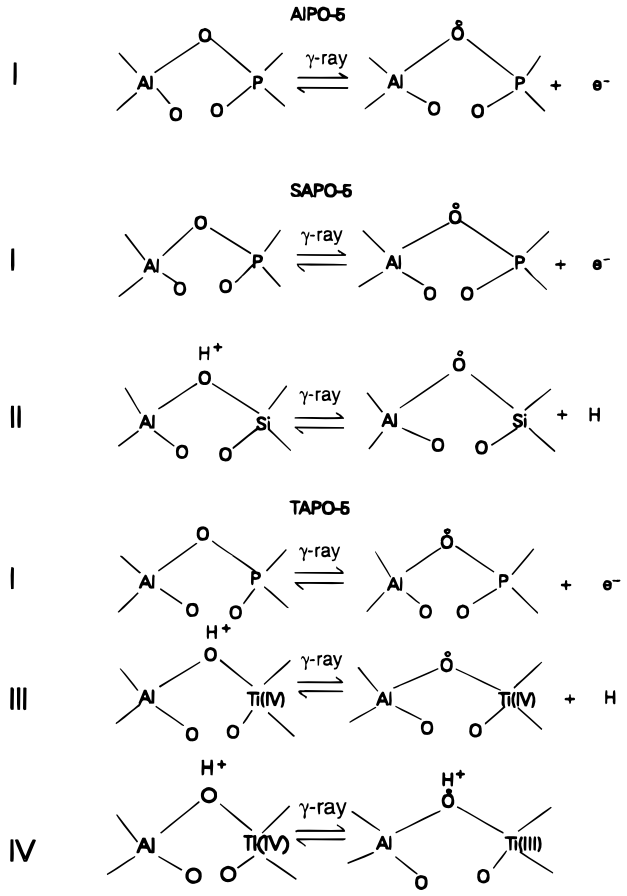

presence of H^+ ions produced by the substitution of tetravalent Si or Ti for a phosphorus site in the AlPO-5 framework (mechanism II and mechanism III). In TAPO-5 another mechanism by which V centers can be stabilized is by reduction of Ti(IV) to Ti(III) using the ejected electron (mechanism IV). This mechanism is consistent with an additional number of V centers observed together with formation of a Ti(III) signal in the ESR spectrum of TAPO-5 in comparison with the spectrum of SAPO-5. This provides indirect evidence for the substitution of titanium in the AlPO-5 framework. On the other hand, no H^+ ions are normally expected for a material where titanium locates in extraframework ion exchangeable sites. In such a case, the formation of V centers by mechanisms III and IV does not occur.

According to the mechanisms proposed here, more than one type of V center may be expected in SAPO-5 and TAPO-5. However, the ESR spectrum for these samples does not distinguish more than one type of V center. This agrees with the previous observations on zeolites, where the various V centers are not distinguishable by ESR, but can be distinguished by their reactivity toward molecular oxygen to form O_2^- ions with different **g** tensors.[17]

Additional evidence for the difference in coordination of Ti between TAPO-5 and TiO_2/SAPO-5 is shown by their behaviors toward CO reduction. The new ESR species observed after reduction of TAPO-5 by CO has a **g** tensor different from that of the Ti(III) species formed by γ-reduction. The difference in the **g** tensors for the two Ti(III) species is attributed to additional interaction of CO molecules with the Ti(III) ions. In TiO_2/SAPO-5 both γ-irradiation and CO reduction produce the same Ti(III) species, but CO reduction is more efficient in producing the T(III) species. The difference in behaviors of TAPO-5 and TiO_2/SAPO-5 suggests a different coordination environment for Ti in the two materials. Four-coordinated titanium in TAPO-5 can have additional coordination with CO, but six-coordinated titanium in TiO_2 nanoparticles on SAPO-5 cannot coordinate with additional CO.

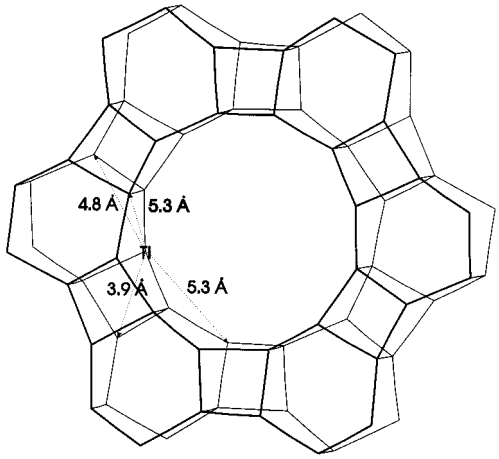

Figure 7. MFI structural model showing the variation in distance between the second-nearest-neighbor tetrahedral sites.

The reaction of molecular oxygen with reduced TAPO-5 and TiO_2/SAPO-5 to produce O_2^- superoxide ions can occur as follows.

$$\mathrm{Ti(III)} + \mathrm{O_2} \rightarrow \mathrm{O_2}^- + \mathrm{Ti(IV)}$$

Although both TAPO-5 and TiO_2/SAPO-5 produce O_2^- ions, the ESR signals have one of their *g* components slightly different from the other. Such a difference has been observed between TS-1 and Ti-exchanged ZSM-5 upon oxygen exposure and has been attributed to a change in the coordination sphere around the Ti centers to which the superoxide binds. In the present case, the deviation is small (from 2.025 to 2.018) as compared to that between TS-1 and Ti−ZSM-5 (from 2.031 to 2.018).[12] The O_2^- ion in TiO_2/SAPO-5 has the same **g** tensor as that observed for Ti−ZSM-5, whereas O_2^- in TAPO-5 and TS-1 has different ones, suggesting different crystal fields for Ti in these two materials.

^{31}P and ^{27}Al ESEM measurements provide other convincing evidence for framework substitution of Ti in TAPO-5. The structure of the AFI framework is given in Figure 7. A titanium ion in a framework P site has four Al atoms as its nearest-neighbor tetrahedral sites. The next-nearest-neighbor tetrahedral sites are occupied by phosphorus atoms which are distributed at various distances between 3.9 and 5.3 Å. There is one phosphorus site at 3.9 Å in the four-ring connecting the Ti site. There are two phosphorus sites at 4.8 Å in the six-ring connecting the Ti site and lying in the plane perpendicular to the *c* axis. The remaining phosphorus sites are at a distance equal to or greater than 5.3 Å. The AFI framework drawn here assumes an average T−O−T distance of 3 Å. In reality, this value is slightly lower since the average Al−O and P−O distances reported for the AlPO-5 framework are 1.71 and 1.48 Å, respectively.[26] Thus, the observed ^{31}P ESEM simulation parameters are consistent with titanium being substituted for a framework phosphorus site. On the other hand, for titanium ion substituting for a framework Al site, there are four nearest-neighbor phosphorus atoms at ∼3 Å. For titanium occupying ion exchangeable sites in the AlPO-5 channel, one would expect three phosphorus atoms at a distance of ∼3.3 Å as observed in several transition-metal exchanged SAPO materials.[27] The strong ^{27}Al modulation observed on the Ti(III) is also an indication of titanium being nearer to aluminum than to phosphorus.

Conclusions

The present ESR and ESEM study on TAPO-5 in comparison with TiO_2/SAPO-5 provides new evidence for the isomorphous substitution of titanium into the aluminophosphate framework. γ-irradiation and CO reduction are both effective in producing T(III) species in TAPO-5. γ-irradiation of activated TAPO-5 produces both Ti(III) ions and V centers. An ESR signal with a rhombic **g** tensor $g_1 = 1.965$, $g_2 = 1.920$, and $g_3 = 1.879$ is assigned to trivalent titanium at a framework site. From a comparative study on the concentration of V centers observed in AlPO-5, SAPO-5 and TAPO-5 after γ-irradiation, possible mechanisms are suggested for the formation of these centers. The large concentration of V centers in TAPO-5 arises from the presence of H^+ ions formed as a result of titanium substituting at a framework phosphorus site. The γ-irradiation of TiO_2/SAPO-5 gives an ESR signal with an axial **g** tensor with $g_\perp = 1.971$ and $g_\parallel = 1.907$ typical of Ti(III) with octahedral symmetry. Upon CO reduction, TiO_2/SAPO-5 produces a Ti(III) species with a similar **g** tensor as that observed after γ-irradiation. However, CO reduction of TAPO-5 gives an ESR signal with a rhombic **g** tensor with $g_1 = 1.969$, $g_2 = 1.954$, and $g_3 = 1.923$ that is different from that for Ti(III) formed by γ-irradiation. The difference seems best explained by additional coordination of tetrahedral framework Ti with CO molecules in TAPO-5 and no such additional coordination for octahedral Ti in TiO_2/SAPO-5. Ti(III) in both TAPO-5 and TiO_2/SAPO-5 readily reacts with molecular oxygen to form O_2^- superoxide ions for which the ESR signals differ in one of their g components and suggest different crystal fields experienced by Ti(III) in these two materials. Simulation of the ^{31}P ESEM spectrum for Ti(III) ions produced after γ-irradiation in TAPO-5 shows one phosphorus atom at 3.9 Å and a two phosphorus atoms at 4.8 Å. These parameters are consistent with titanium substituting for framework phosphorus sites.

Acknowledgment. This research was supported by the National Science Foundation and the Robert A. Welch Foundation.

References and Notes

(1) Notari, B. *Adv. Catal.* **1996**, *41*, 253.
(2) Reddy, J. S.; Kumar, R.; Ratnasamy, P. *Appl. Catal.* **1990**, *58*, L1.
(3) Serrano, D. P.; Li, H. X.; Davis, M. E. *J. Chem. Soc., Chem. Commun.* **1992**, 745.
(4) Camblor, M. A.; Corma, A.; Martinez, A.; Perez-Pariente, J. *J. Chem. Soc., Chem. Commun.* **1992**, 589.
(5) Ulagappan, N.; Krishnasamy, V. *J. Chem. Soc., Chem. Commun*. **1995**, 373.
(6) Zahedi-Niaki, M. H.; Joshi, P. N.; Kaliaguine, S. In *Progress in Zeolite and Microporous Materials*; Chon, H., Ihm, S.-K., Uh, Y. S., Eds.; Studies in Surface Science and Catalysis, Vol. 105; Elsevier: Amsterdam, 1997; p 1013.
(7) Corma, A.; Camblor, M. A.; Esteve, P.; Martinez, A.; Perez-Pariente, J. *J. Catal.* **1994**, *145*, 151.
(8) Koyano, K. A.; Tatsumi, T. In *Progress in Zeolite and Microporous Materials*; Chon, H., Ihm, S.-K., Uh, Y. S., Eds.; Studies in Surface Science and Catalysis, Vol. 105; Elsevier: Amsterdam, 1997; p 93.
(9) Kuznicki, S. M. U.S. Patent 4 853 202, 1989.
(10) Kuznicki, S. M. U. S. Patent 4 938 939, 1990.
(11) Dyrek, K.; Che, M. *Chem. Rev. (Washington, D.C.)* **1997**, *97*, 305.
(12) Tuel, A.; Diab, J.; Gelin, P.; Dufaux, M.; Dutel, J.-F.; Tarit, Y. B. *J. Mol. Catal.* **1990**, *63*, 95.
(13) Kevan, L. *Acc. Chem. Res.* **1987**, *20*, 1.
(14) Martens, J. A.; Mertens, M.; Grobet, P. J.; Jacobs, P. A. In *Innovation in Zeolite Materials Science*; Grobet, P. J., Mortier, W. J., Vansant, E. F., Schulz-Ekloff, G., Eds.; Studies in Surface Science and Catalysis, Vol. 37; Elsevier: Amsterdam; 1988; p 95.
(15) Xu, Y.; Langford, C. H. *J. Phys. Chem. B* **1997,** *101*, 3115.
(16) Anderson, M. W.; Kevan, L. *J. Chem. Soc., Faraday Trans.* **1987**, *83*, 3505.
(17) Abou-Kais, A.; Vedrine, J. C.; Massardier, J. *J. Chem. Soc., Faraday Trans.* **1975**, *71*, 1697.
(18) Abou-Kais, A.; Vedrine, J. C.; Massardier, J.; Dalmai-Imelik, G.; Imelik, B. *J. Chem. Phys*. **1972**, *69*, 561.
(19) Che, M.; Tench, A. J. *Adv. Catal.* **1983**, *32*, 1.
(20) Kanzig, W.; Cohen, M. H. *Phys. Rev. Lett.* **1959**, *3*, 509.
(21) Lee, S.; Bray, P. J. *J. Chem. Phys.* **1964**, *40*, 2982.
(22) Lunsford, J. H. *Adv. Catal*. **1972**, *22*, 265.
(23) Naccache, C.; Tarit, Y. B. *Trans. Faraday Soc.* **1973**, *69*, 1475.
(24) Iyengar, D.; Codell, M.; Karra, J. S.; Turkevich, J. *J. Am. Chem. Soc.* **1966**, *88*, 5055.
(25) Prakash, A. M.; Kevan, L., unpublished result.
(26) Bennett, J. M.; Cohen, J. P.; Flanigen, E. M.; Pluth, J. J.; Smith, J. V. In *Intrazeolite Chemistry*; Stucky, G. D., Dwyer, F. G., Eds.; ACS Symp. Ser. 218; American Chemical Society: Washington, DC, 1983; p 109.
(27) Prakash A. M.; Wasowicz, T.; Kevan, L. *J. Phys. Chem.* **1996**, *100*, 15947.